

Design Parameters of Solid Oxide Fuel Cell Microstructure Based on Power Generation Performance Simulation

Jai-Houng Leu,^{1*} Ay Su,^{2**} Shun-Chi Kuo,³
Li-Hsing Fang,⁴ Kuang-Chung Chen,¹ and Tian-Syung Lan⁵

¹School of Computer Science, Weifang University of Science and Technology,
Weifang City, Shandong Province, China

²Yuan Ze University, Taoyuan County, 32003, Taiwan, R.O.C.

³Department of Mechanical and Industrial Engineering, Vanung University, Taoyuan City, 32003, Taiwan, R.O.C.

⁴Department of Mechanical Engineering, Nanya Institute of Technology,
Zhongli District, Taoyuan City, 320, Taiwan, R.O.C.

⁵Department of Information Management, Yu-Da University of Science and Technology,
Miaoli County, Taiwan, R.O.C.

(Received November 11, 2024; accepted April 11, 2025)

Keywords: power generation, simulation, URSOFC, electrode

By building a model using COMSOL Multiphysics® software, we determined the design parameters for utilizing the microstructure of unitized solid oxide fuel cell (URSOFC). Numerical simulations were performed with these parameters using governing equations. We found that the effects of cathode porosity and average pore size on the power generation of URSOFC were significant, and that the effects of anode porosity and average pore size were negligible. Our results revealed that the higher the concentration of water vapor, the higher the efficiency of hydrogen production, and the lower the permeability, the worse the performance. The cathode material must be selected on the basis of porosity, pore size, and permeability.

1. Introduction

When studying combustion,⁽¹⁾ chemical processes,⁽²⁾ and microelectronics to understand electrochemical complexity, CHEMKIN or Cantera software is widely used because they are designed to solve complex chemical kinetic problems. By exploring the complexity of electrochemistry represented by multistep elementary charge transfer reactions, supporting ion and electron transport, new materials and related processing technologies can be improved. The rates of global charge transfer reactions follow the Butler–Volmer approximation.⁽¹⁾ Common principles of electrochemistry are the basis for the design and implementation of software to explore material properties and their applications.

Qin *et al.*⁽³⁾ proposed that water management is one of the key issues in the design and optimization of fuel cells, and it has been extensively studied using experiments and numerical simulations over the past few decades. In a proton exchange membrane fuel cell, the membrane must have sufficient moisture to ensure high proton conductivity. On the other hand, owing to the lower working temperature and the water generated, excessive humidification will lead to

*Corresponding author: e-mail: jahonleu@yahoo.com.tw

**Corresponding author: e-mail: meaysu@saturn.yzu.edu.tw

<https://doi.org/10.18494/SAM5473>

excessive water accumulation in the cathode structure, which can subsequently block the cathode gas flow path. The result of this phenomenon is that the blocked channel is in a parallel flow path configuration with a lower air velocity, resulting in more water accumulation in the interrupted channel, thus reducing the performance of the battery. The higher pressure drop will block the flow channel of the serpentine flow channel plate; then, the cathode consumes higher parasitic energy and reduces the overall performance of the system. Therefore, proper water management must be implemented to improve the performance of proton exchange membrane fuel cells.

Jang *et al.*⁽⁴⁾ proposed that fuel cells be tested on the basis of numerical models with optimized geometric parameters. On the basis of computational fluid dynamics and the optimization design and optimization algorithms of the obtained geometric parameters, we found that the optimal position to maximize the average current density of the bipolar plate placed in the flow channel is the interdigitated flow field. It is also the best position to maximize the average current density between many geometries such as parallel, serpentine, and interdigital flow channels in their study. There are many sharp turns in the traditional flow channel, where large pressure drops occur in the flow field. Spiral or meandering channels can be an alternative to the traditional flow channel. However, the parallel, serpentine, and interdigital flow channels can be used instead of the traditional flow channel.

The parameters must be determined experimentally, but very few kinetic parameters can be obtained from relevant material databases.⁽⁵⁾ However, conducting experiments in the closed systems of batteries and fuel cells is challenging, especially because there are numerous different physical parameters that can affect their electrochemical processes. To accurately determine the kinetic parameters, it is necessary to conduct both experiments and simulations simultaneously. For batteries and fuel cells, cyclic voltammetry and electrochemical impedance spectroscopy (EIS or AC impedance) are used in the simulations.⁽⁶⁾

Microactuator fuel cells are a prominent clean energy source and a step towards developing self-powered systems in indoor and outdoor environments.⁽⁷⁾ Electrochemical kinetic theory and secondary current distribution models are applied in fuel cell research. In these models, charge transfer mechanisms and activation are studied as they affect the electrochemical reactions of fuel cells. Simulation results using these models provide the operating voltage and current of fuel cells, thereby enabling the selection of appropriate electrode and electrocatalyst materials, as well as the activation overpotential losses during heat conduction.

Therefore, we built a model to determine the parameters using the governing equations. These parameters are very important for developing the sensor technology used in fuel cells. During the operation of fuel cells, various sensors are used to monitor and regulate temperature, pressure, humidity, hydrogen and oxygen input, gas flow, and conductivity. These sensors provide real-time data to optimize the performance of fuel cells. Therefore, the results of this study provide a reference for the development and improvement of sensors used in fuel cells and secondary batteries, as well as the performance of fuel cells.

2. Background Knowledge

The structure of the unitized regenerative solid oxide fuel cell (URSOFC) used in this study is shown in Fig. 1.

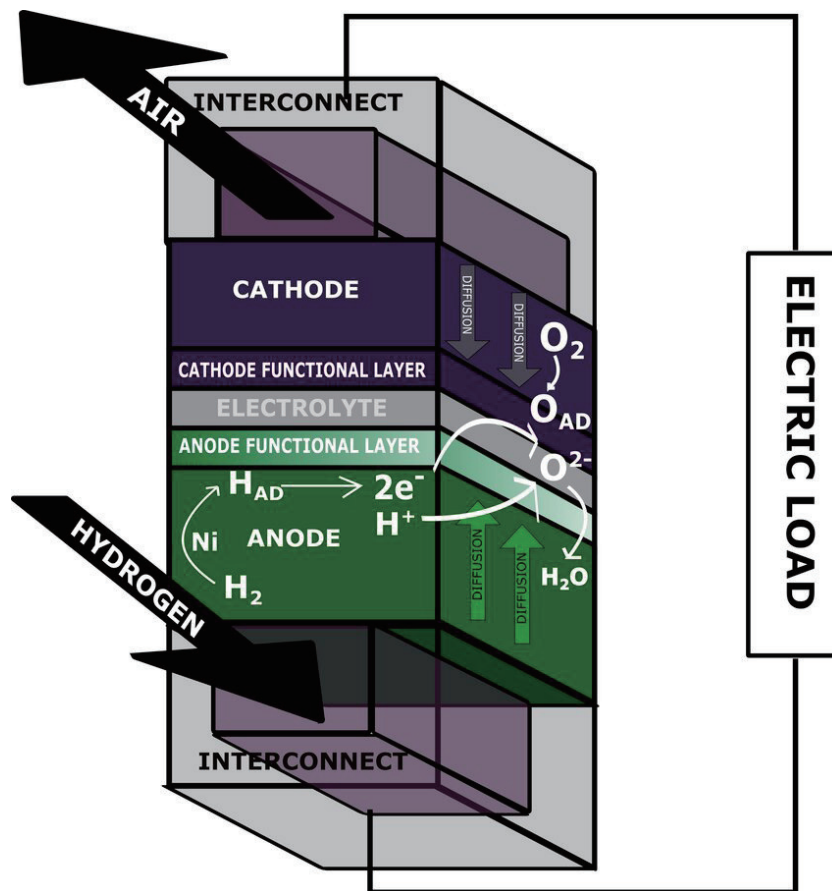


Fig. 1. (Color online) Structure of solid electrolyte hydrogen fuel cell.

3. Numerical Model

3.1 Mathematical model

The numerical model of the respiratory proton exchange membrane fuel cell in this study mainly describes the flow field using the equations of the conservation of mass, momentum, energy, and current. The electrochemical reactions that occur in the catalyst layer are described by the Butler–Volmer equation. The electrode overpotential of the pore electrode in the catalyst layer is calculated using the DC conduction equation of electrons and ions. In this study, the computational area is divided into many computational grids with control volumes, and the algebraic equations on the computational grids are discretized into computational grids, so that the calculations can be performed on a computer. The domination equation is divided into the following three parts:

(1) Transport of pure fluid in the flow field

Pure fluids are mainly used to describe the transport phenomena of gases in the flow channel, including the equations for the conservation of mass, momentum, and concentration.

(2) Transmission in porous materials

The mass and momentum conservation equations of porous materials include the gas diffusion layer, catalyst layer, and proton exchange membrane, which are affected by the porosity ε and permeability κ .

(3) Electrochemical reactions in the catalyst layer

The transmission current $J_{T,j}$ can be obtained using the Butler–Volmer equation and written in the following form:

$$J_{T,j} = \frac{j_{0,j}}{\prod_{k=1}^N [\Lambda_{k,ref}]^{\alpha_{k,j}}} \left[\exp\left(\frac{\alpha_{a,j} F}{RT} \eta\right) - \exp\left(-\frac{\alpha_{c,j} F}{RT} \eta\right) \right] \times \prod_{k=1}^N [\Lambda_k]^{\alpha_{k,j}}. \quad (1)$$

In Eq. (1), $j_{0,j}$ is the reference current of the open circuit voltage, and $\alpha_{a,j}$ and $\alpha_{c,j}$ are the positive transmission number anode transfer coefficient and the negative transmission number cathode transfer coefficient, respectively. $[\Lambda_k]$ is the average molar concentration of the k th reactive element, N is the number of reactive elements, $\alpha_{k,j}$ is the concentration index of the k th element during the reaction in step j , and η is the potential difference between the ion potential ΦF and the electron potential ΦS . A nonlinear equation for the interface between pores and contact media can be obtained by combining the relevant equations, and the Y_i values of all elements can be solved by numerical analysis.

The numerical model created in this study was used to establish the 3D model shown in Fig. 2. In this type of 3D model, the 1D and 2D models can be observed, the lack of the mass transfer effect and ohmic impedance can also be observed, and the internal flow field, mass transfer, electric field, and chemical phenomena of the breathing proton exchange membrane fuel cell can be further explored.

3.2 Simulation parameters

COMSOL Compiler™ (version 5.4) was used to generate a simulation application independently in this study. The parameters of this simulation are set as porosity (0.6), the average pore size inside the electrode (1 μm), the internal permeability of the electrode ($1 \times 10^{-12} \text{ m}^2$), the effective surface area of the electrode (1000 /m), and the equivalent ratio (3 for anode and 5 for cathode) at the initial operating temperature (1000 °C).

The results to be obtained in this study are the effects of different design parameters related to the electrode microstructure on the performance of fuel cells after the computer numerical simulation.

4. Simulation Results

Figure 3 shows that the higher the water vapor concentration, the higher the hydrogen production efficiency. The more water vapor, the more hydrogen can be produced because the hydrogen mainly comes from the electrolysis of water vapor.

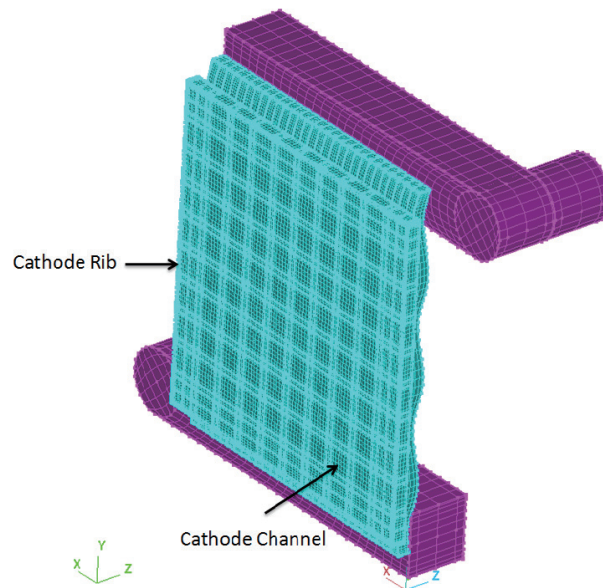


Fig. 2. (Color online) 3D simulation model of the cathode stereogram.

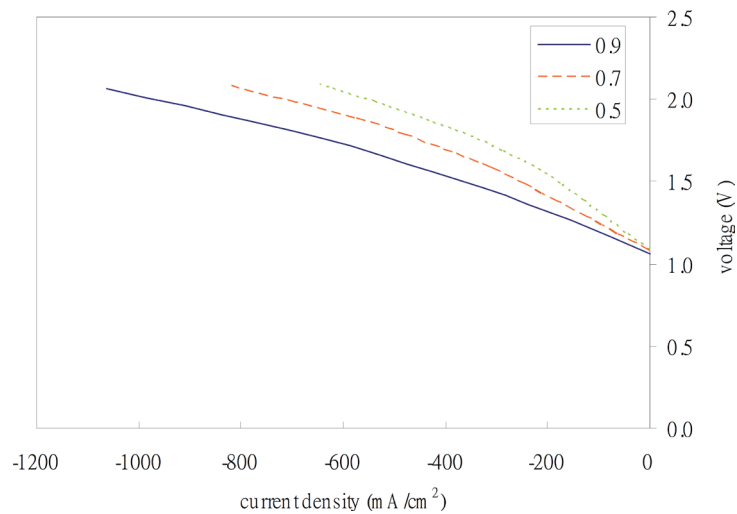


Fig. 3. (Color online) Effect of different water vapor inlet concentrations on hydrogen production.

Figure 4 shows that the performance of URSOFC improves with increasing porosity. The effect of cathode porosity on URSOFC performance is greater than that of anode porosity. The cathode porosity significantly affects the hydrogen production efficiency, whereas the anode porosity has no significant effect.⁽⁸⁾ When the anode porosity increases, the efficiency also increases, but after exceeding 0.4, the performance does not improve further.

Figure 5 shows the effect of cathode permeability on URSOFC power generation. The lower the permeability, the worse the performance because the reduction in permeability inhibits gas

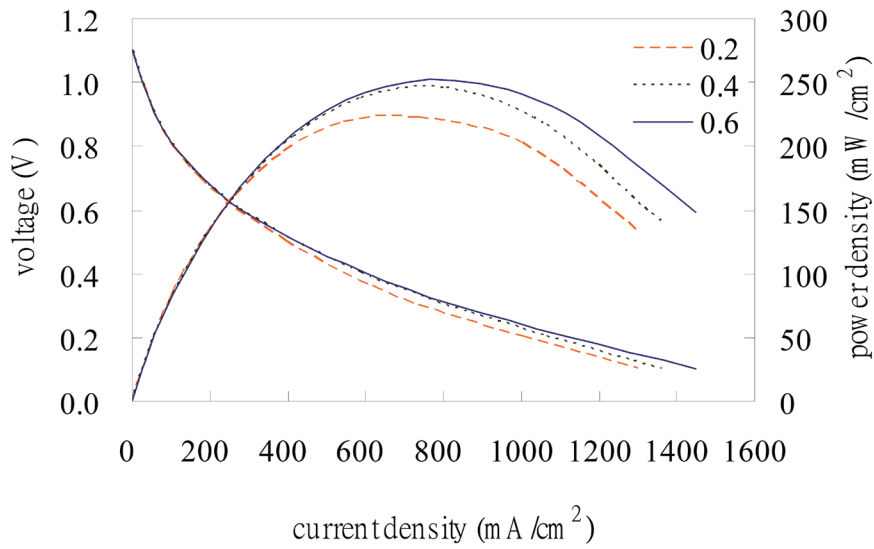


Fig. 4. (Color online) Effect of cathode porosity on power generation.

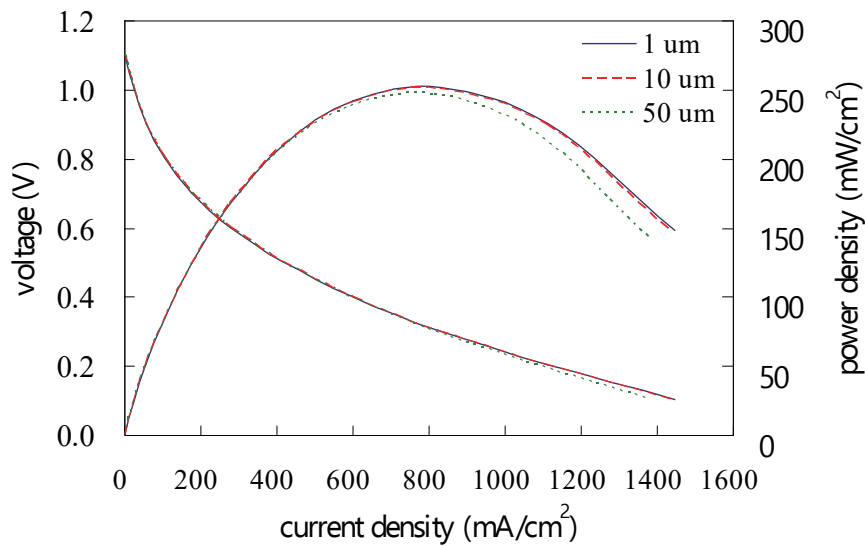


Fig. 5. (Color online) Effect of average pore size of cathode on power generation.

convection inside the electrode, thus reducing performance. Figure 6 shows that the average pore size of the anode has little effect on the performance, except that it has a significant impact on the performance when the pore size of the cathode is less than 50 μm .

Thermiculite-866 showed a higher cyclability in solid oxide fuel cell (SOFC) thermal cycling experiments than AFS-170. Mass loss and thermogravimetric analysis (TGA) techniques were performed on Thermiculite-866 and AFS-170 alumina felts used as SOFC seals under humidified conditions. The alumina felts were not affected at 800 $^{\circ}\text{C}$ in inert, oxidizing, and reducing

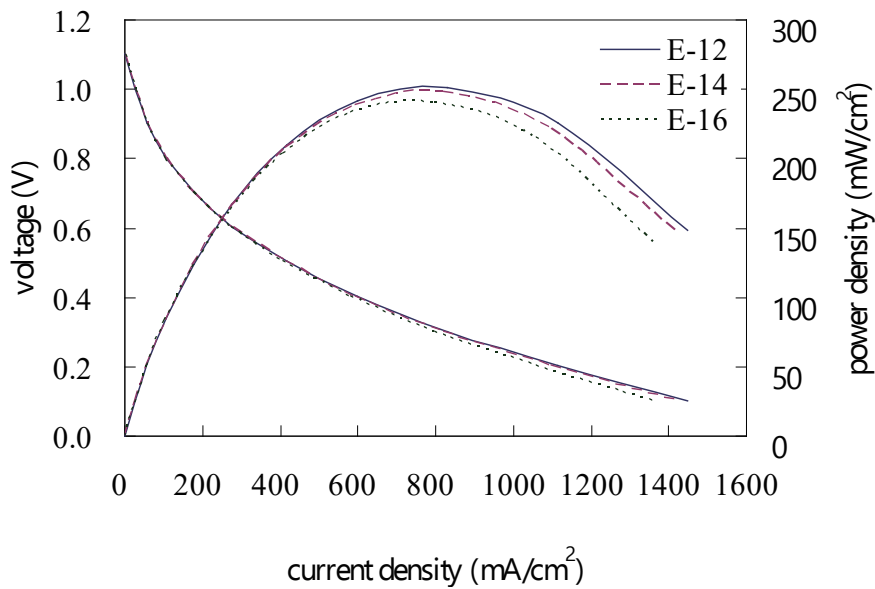


Fig. 6. (Color online) Effect of cathode permeability on power generation.

atmospheres, whereas Thermiculite-866 showed reversible redox. This indicates that the properties of the cathode and anode materials are very important to the performance of SOFCs.⁽⁹⁾

The performance characteristics of lanthanum strontium ferrite (LSF) and lanthanum strontium cobalt ferrite (LSCF) are higher than those of lanthanum strontium manganite (LSM) and LSCF. The LSF can operate stably for a long time because of its higher ion conductivity.⁽²⁾ The effects of porosity and pore size on fuel cell performance can be improved because the material has a higher conductivity and/or a more stable thermal stress resistance.

5. Conclusions

The higher the concentration of water vapor, the higher the efficiency of hydrogen production. The anode porosity and average pore size have limited effects. Permeability also affects power generation. In contrast, the higher the cathode porosity and the larger the average pore size, the higher the power generation. To improve the power generation of URSOFC, its cathode material must be selected considering porosity, pore size, and permeability.

The higher the cathode porosity and the larger the average pore size, the more significant the increase in power generation in the power generation mode, which is completely different from that in the hydrogen production mode. The lower the cathode permeability, the worse the performance in the power generation mode in this study. The effects of anode porosity and average pore size are negligible, which is the same as that in the hydrogen production mode.

However, depending on the inlet water vapor content, increasing the cathode porosity and average pore size at the operating temperature is very important to corrosion resistance for its severe degradation. Further investigation of the optimal parameters (cathode porosity and average pore size) of other materials is necessary to maximize the power generation of URSOFC.

References

- 1 S. C. DeCaluwe, P. J. Weddle, H. Zhu, A. M. Colclasure, W. G. Bessler, G. S. Jackson, and R. J. Kee: *J. Electrochem. Soc.* **165** (2018) E637. <https://doi.org/10.1149/2.0241813jes>
- 2 Y. L. Liu, K. Thydén, M. Chen, and A. Hagen: *Solid State Ionics* **206** (2011) 97. <https://doi.org/10.1016/j.ssi.2011.10.020>
- 3 Y. Qin, Q. Du, Y. Yin, K. Jiao, and X. Li: *J. Power Sources* **222** (2013) 150. <https://doi.org/10.1016/j.jpowsour.2012.07.084>
- 4 J. Y. Jang, C. H. Cheng, W. T. Liao, Y. X. Huang, and Y. C. Tsai: *Appl. Energy* **99** (2012) 67. <https://doi.org/10.1016/j.apenergy.2012.04.011>
- 5 T. Henriques, B. César, and P. J. C. Branco: *Appl. Energy* **87** (2009) 1400. <https://doi.org/10.1016/j.apenergy.2009.09.001>
- 6 Q. Zhao and F. C. Lee: *IEEE Trans. Power Electron.* **18** (2003) 65. <https://doi.org/10.1109/TPEL.2002.807188>
- 7 E. O. de la Rosa, J. V. Castillo, M. C. Campos, G. R. B. Pool, G. B. Nuñez, A. C. Atoche, and J. O. Aguilar: *Sensors* **19** (2019) 1378. <https://doi.org/10.3390/s19061378>
- 8 J. H. Leu, Y. Zhang, A. Su, and T. S. Lan: *Proc. 2021 IEEE 3rd Eurasia Conf. Biomedical Engineering, Healthcare and Sustainability (IEEE, 2021)*. <https://doi.org/10.1109/ECBIOS51820.2021.9510307>
- 9 J. Aicart, J. Kuhn, and O. Kesler: *Fuel Cell* **17** (2017) 90. <https://doi.org/10.1002/fuce.201600110>